

Adaptive Graph Convolutional Networks for Weakly Supervised Anomaly Detection in Videos

Congqi Cao, Xin Zhang, Shizhou Zhang, Peng Wang, and Yanning Zhang

Abstract—For weakly supervised anomaly detection, most existing work is limited to the problem of inadequate video representation due to the inability of modeling long-term contextual information. To solve this, we propose a novel weakly supervised adaptive graph convolutional network (WAGCN) to model the complex contextual relationship among video segments. By which, we fully consider the influence of other video segments on the current one when generating the anomaly probability score for each segment. Firstly, we combine the temporal consistency as well as feature similarity of video segments to construct a global graph, which makes full use of the association information among spatial-temporal features of anomalous events in videos. Secondly, we propose a graph learning layer in order to break the limitation of setting topology manually, which can extract graph adjacency matrix based on data adaptively and effectively. Extensive experiments on two public datasets (i.e., UCF-Crime dataset and ShanghaiTech dataset) demonstrate the effectiveness of our approach which achieves state-of-the-art performance.

Index Terms—Anomaly detection, temporal modeling, graph convolutional networks, adaptive learning.

I. INTRODUCTION

WITH the growing popularity of surveillance cameras and the increasing awareness of security in public places, there is an urgent need to develop a technology that can automatically detect and raise alarms for abnormal events in surveillance video [1], [2], [3]. Events in the real world are complex and diverse. Meanwhile, fine-grained annotation of training sets takes a lot of time and effort. Hence, weakly supervised anomaly detection (WSAD) becomes a popular research field. In previous work, WSAD has been formulated as a Multiple Instance Learning (MIL) task [2], [4], [5], [6]. Sultani et al. [2] constructed a large-scale anomaly dataset and proposed a deep MIL ranking model to detect anomalies. Wan et al. [5] improved this framework by replacing the max anomaly score selection policy with a k -max value selection policy. Yu et al. [7] proposed an effective cross-epoch learning strategy to introduce additional information from previous training epochs, which is compatible to most previous WSAD frameworks. However, the above methods ignore the spatial-temporal connection among video segments.

This work was supported by the National Natural Science Foundation of China under Grant U19B2037 and Grant 61906155, and the Ministry of Science and Technology Foundation funded project under Grant 2020AAA0106900.

Congqi Cao, Xin Zhang, Shizhou Zhang, Peng Wang and Yanning Zhang are with the National Engineering Laboratory for Integrated Aero-Space-Ground-Ocean Big Data Application Technology, School of Computer Science, Northwestern Polytechnical University, Xi'an 710129, China (e-mail: {congqi.cao, szzhang, peng.wang, ynzhang}@nwpu.edu.cn; zhangxin_@mail.nwpu.edu.cn).

In recent years, several works have applied graph convolutional networks (GCNs) [8], [9], [10], [11] over the graph to model relations among different nodes and learn powerful video representations. Zhong et al. [12] used GCN to denoise normal segments in anomalous videos, and trained an action classifier with the obtained pseudo-labels. However, during the testing phase, the model only used current information despite capturing long-range temporal dependencies of the full video in the training phase. And the denoising process may clean up the anomalies, resulting in information loss. Wu et al. [13] proposed a GCN with three parallel branches capturing long-range dependencies, local positional relation and the proximity of the predicted scores to describe different relationships among video segments respectively. However, three independent branches cannot model complex relationships coupled together in the video effectively and lead to slow iterative optimization. In addition, there are no learnable parameters in the adjacency matrix of the graph, hence the defined graphs may not be suitable for specific anomaly detection tasks.

In summary, we observe the following challenges in using GCN to model temporal contextual information for WSAD: (1) Only one network structure is used to model one type of relationship, or multiple independent branches are used to model different types of relationships separately, which cannot model multiple relationships coupled together within a sequence effectively. (2) Existing GCN methods ignore the fact that predefined graph structures are not optimal and it could be updated during the training process. In this paper, we propose an adaptive GCN to overcome these challenges. Our framework is shown in Figure 1. For challenge 1, we use temporal consistency graph to describe the intrinsic association relationships of features in a smooth undulating interval. And we use feature similarity graph to express the intrinsic association relationships of video segment features within the same event. However, both single temporal consistency GCN and single feature similarity GCN are not optimal to anomalous event detection. In order to make better use of the intrinsic correlations among segments, we integrate the two perspectives to jointly construct a global graph for spatial-temporal feature learning of events. For challenge 2, during the construction of the adjacency matrix, we break the limitation of manual setting. We consider the similarity among spatial-temporal features of video segments and other potential contextual semantic relationships to learn a video content-adaptive graph adjacency matrix that can be trained with the whole network simultaneously. As far as we know, we are the first to learn a global video content-adaptive graph adjacency matrix to model the contextual relationships among

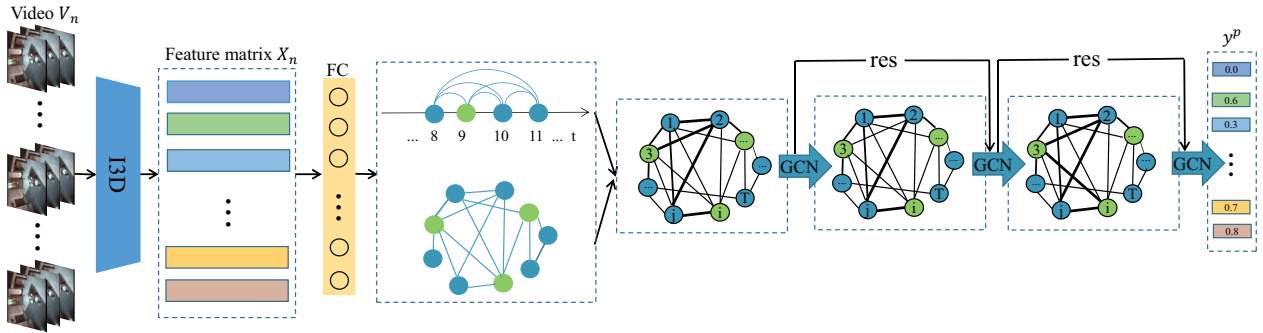


Fig. 1. Our proposed WAGCN receives a $T_n \times D$ feature matrix X_n extracted from video V_n . Then, we construct a global graph to capture the long and short-range temporal dependencies among segment features. Next, we train adaptive GCN using the top- k largest anomaly probability scores from abnormal and normal videos.

video segments for WSAD. Moreover, vanilla GCN suffers from over-smoothing problem, where the representations of all nodes converge to a smooth point, making them independent of the input features and causing the gradient to vanish. We adopt to add residual connection [14] in GCN to solve this problem for WSAD. In summary, our main contributions are as follows:

1) We propose to construct a global graph based on the similarity of spatial-temporal features and temporal proximity of video segments to better exploit the intrinsic correlation relationships among segments.

2) We propose to learn an adaptive adjacency matrix of the graph in an end-to-end manner to increase the flexibility of the model. And we propose an effective way to improve the learning ability of GCN by introducing residual connection.

3) Our proposed method achieves 84.67% and 96.05% frame-level AUC on UCF-Crime and ShanghaiTech datasets, outperforming the existing state-of-the-art methods.

II. PROPOSED METHOD

A. Feature Extraction

The training set has N training videos $\{V_n\}_{n=1}^N$ and corresponding weakly supervised labels $\{y_n\}_{n=1}^N$, where $y_n \in \{0, 1\}$. Among which, $y_n=1$ indicates that V_n contains at least one anomalous segment, but no temporal location annotation is provided. $y_n=0$ means that V_n is entirely comprised of normal segments. Following the earlier MIL-based anomaly detection method [2], the video V_n is divided into T_n non-overlapping segments containing 16 frames before each V_n is fed to the feature extractor. The Inflated 3D (I3D) [15] pretrained on the Kinetics dataset is used as the feature extraction network to extract the appearance and motion information of the video. The feature matrix X_n is composed of features from video V_n . The dimension of X_n is $T_n \times D$, where D denotes the dimension of segment features.

B. Graph Construction Module

Anomalous events occur in a continuous period of time and have a consistent behavior pattern over a period of time. Thus, in order to better model the temporal relationship of the video and better express the dynamic characteristics of the video,

we combine the similarity of video segments' spatial-temporal features and the degree of video segments' temporal proximity to construct graph.

1) *Feature similarity graph*: Features from the feature extractor first go through a fully connected layer to decrease the feature dimension, in order to mitigate the curse of dimensionality. We propose to construct a feature similarity graph G^F with graph learning layer to represent the similarity among segments adaptively. We aim at capturing dynamic spatial-temporal dependencies. In other words, instead of defining the weights of two connected nodes based on the node inputs directly, we dynamically adjust them as the model is trained.

We represent the pairwise relations between every two segments in the graph as follows. Since an adjacency matrix should be non-negative, we bound the similarity to the range of $(0, 1]$ with a normalized exponential function. Therefore, the adjacency matrix A^F is defined as:

$$A^F = \text{SoftMax}(\text{relu}(XW_1)\text{relu}(W_2^T X^T)) \quad (1)$$

where W_1 and W_2 are $d \times d$ dimensional weights which are learnable via back propagation. As a result, the elements of A^F are parameterized and optimized along with the other parameters during the training process.

2) *Temporal consistency graph*: For most anomalous videos, not all anomalous segments are similar to explosive events which happen so drastically. Instead, they require an undulating process time. As pointed out in [16], [17], [18], temporal consistency contributes to many video-based tasks. The temporal consistency graph G^T is built directly based on the temporal structure of the video. Its adjacency matrix $A^T \in R^{N \times N}$ depends on the temporal position of the i -th and j -th segments:

$$A_{ij}^T = \exp(-|i - j|) \quad (2)$$

i.e., for the j -th segment, the closer it is to the i -th segment, the greater the weight assigned to their edge, which can better reflect the influence of a segment on another.

C. Graph Convolutional Module

To explore and exploit relationships among segments, we use GCN to model the relationships among segments. Specifi-

cally, for the k -th layer, the graph convolution is implemented by

$$X^k = \sigma \left((A^F + A^T) X^{k-1} W^k \right) + X^{k-1} \quad (3)$$

where $X^{k-1} \in R^{N \times d_{k-1}}$ are the hidden features for all segments at layer $k-1$, and d_{k-1} is the dimension of features. $W^k \in R^{d_{k-1} \times d_k}$ is a trainable parametric matrix, and σ represents the activation function.

In addition, we add residual connections between adjacent layers inspired by ResNet [14] and use summation for aggregation, which is plug-and-play i.e., can be inserted into any existing model without destroying its initial behavior. If the dimension of the input channel is different from the number of output channels, a 1×1 convolution is inserted in the residual path to transform the input to match the output in the channel dimension.

D. Training Loss of the Proposed Algorithm

As mentioned before, each video only has a normal or abnormal video-level label. Obviously, segments with large abnormal scores in the abnormal video is more likely to be abnormal segments, while segments with large abnormal score in the normal segment is still normal segments. In order to expand the inter-class distance between abnormal and normal segments under weak supervision, we use k -max loss function [5]. Specifically, given the abnormal score $s = \{s_i\}_{i=1}^T$ of video V , we choose the top- k elements in s denoted as $S = \{s_i\}_{i=1}^k$, where $k = \lfloor \frac{T}{8} + 1 \rfloor$. The final classification loss is the binary cross-entropy between the predicted label and the ground truth of the training video, which is given by:

$$L_{k\text{-max}} = \frac{1}{k} \sum_{s_i \in S} [-y \log(s_i) + (1 - y) \log(1 - s_i)] \quad (4)$$

III. EXPERIMENT RESULTS

A. Datasets

1) *UCF-Crime*: UCF-Crime is a large-scale dataset consisting of long untrimmed surveillance videos [2]. It covers 13 real-world anomalies, including Abuse, Arrest, Arson, Assault, Accident, Burglary, Explosion, Fighting, Robbery, Shooting, Stealing, Shoplifting, and Vandalism. All videos are divided into two parts: the training set consisting of 800 normal and 810 anomalous videos, and the testing set including the remaining 150 normal and 140 anomalous videos.

2) *ShanghaiTech*: ShanghaiTech is a medium-sized dataset containing 437 videos, with an average of 726 frames per video. The dataset includes 130 abnormal events in 13 scenes collected at ShanghaiTech University, with complex lighting conditions and camera angles. In order to make it suitable for evaluating weakly supervised binary classification methods, Zhong et al. [12] split the data into two subsets: the training set which is made up of 175 normal and 63 anomalous videos, and the test split which contains 155 normal and 44 anomalous videos.

B. Evaluation Metrics

Following previous work, we use the frame-level receiver operating characteristic curve (ROC) and corresponding area under the curve (AUC@ROC) to evaluate the performance of our proposed method and comparison methods.

C. Implementation Details

In this work, 2048-D features are extracted from the ‘‘mix 5c’’ layer of I3D. The length of the videos varies widely, ranging from seconds to hours. Directly processing a very long video is not practical due to GPU memory constraints. Therefore, if the length T_n of the video V_n is less than a predefined length T , we will process the whole video. Otherwise, we uniformly extract T segments from the video to represent the entire video. In this paper, we set T to 150 for UCF-Crime and 100 for ShanghaiTech. The FC layer described in the model have 512 nodes, and the GCN layers described in the model have 128, 32 and 1 nodes, where each of those layers except the last layer is followed by a ReLU activation function and a dropout function with a dropout rate of 0.6. The last layer is followed by a Sigmoid activation function. Our method is trained in an end-to-end manner using the Adam optimizer with a weight decay of 0.0005 and a batch size of 64 for 100 epochs. The learning rate is set to 0.001. Each mini-batch consists of 32 samples from randomly selected normal and abnormal videos.

D. Experimental Results and Discussions

We compare our method with the existing state-of-the-art methods on two datasets. The results are shown in Table 1. On UCF-Crime, our method outperforms MIST [6] by 2.37%, XELM [7] by 2.52%, and BN-SVP [19] by 1.28%. Noticeably, using the same I3D-RGB features, our method shows a significant improvement over the previous GCN-based methods, outperforming Zhong et al. [12] by 3.59% and Wu et al. [13] by 2.23%. Furthermore, our method even outperforms the supervised method [20] by 2.67%, which adds temporal and spatial labels to the UCF-Crime dataset and trains Convolutional 3D Network [21] with Non-local Network (NLN) [22] for anomaly detection. On ShanghaiTech dataset, our method achieves better performance compared to previous weakly supervised methods [2], [4], [23], [24]. Especially, our method outperforms GCN-based weakly supervised method [12] by a significant margin of 19.61%, which indicates that our GCN module can capture the temporal dependence more effectively. Our method also improves the performance over AR-Net [5] by 4.81% even though it uses additional multimodal features.

To further illustrate the performance of our model, we visualize the temporal predictions of the model. As shown in Figure 2, our model is able to respond to both normal and abnormal events accurately.

E. Ablation Study

To demonstrate the effect of sampling length, we vary the value of sampling length on UCF-Crime and plot the results in

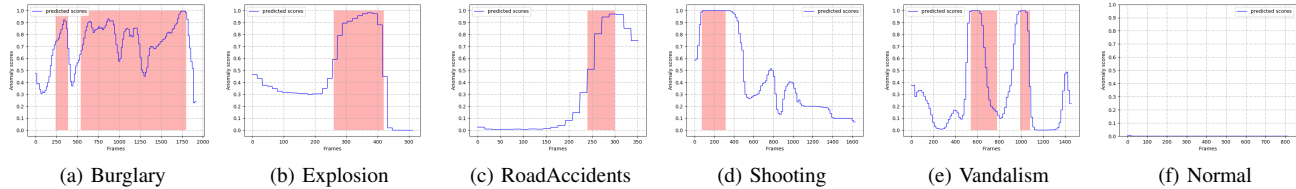


Fig. 2. Visualization of the testing results on UCF-Crime. The red blocks in the graphs are temporal ground truths of anomalous events.

TABLE I

AUC(%) PERFORMANCE COMPARISON. THE RESULTS WITH † ARE RE-IMPLEMENTED WITH I3D FEATURES.

Method	Source	Feature	UCF-Crime	ShanghaiTech
Sultani et al. [2]	CVPR18	C3D RGB	75.41	83.17
Sultani et al. [2]†	CVPR18	I3D RGB	76.92	85.32
Zhang et al. [4]	ICIP19	C3D RGB	78.66	82.50
Motion-Aware [23]	BMVC19	PWC Flow	79.00	/
Liu et al. [20]	MM19	C3D RGB	70.10	/
Liu et al. [20]	MM19	NLN RGB	82.00	/
Zhong et al. [12]	CVPR19	C3D RGB	81.08	76.44
AR_Net [5]†	ICME20	I3D RGB	78.96	85.38
AR_Net [5]†	ICME20	I3D RGB	/	91.24
SRF [24]	SPL20	I3D RGB	79.54	84.16
Wu et al. [13]	ECCV20	I3D RGB	82.44	/
CLAWS [25]	ECCV20	C3D RGB	83.03	89.67
MIST [6]	CVPR21	I3D RGB	82.30	94.83
XELM [7]	SPL21	I3D RGB	82.15	87.83
BN-SVP [19]	CVPR22	I3D RGB	83.39	96.00
Ours	/	I3D RGB	84.67	96.05

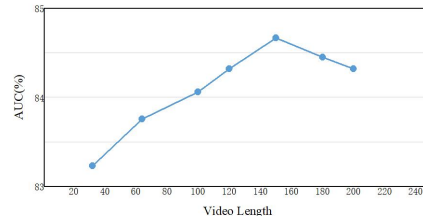


Fig. 3. Performance of different sampling lengths on UCF-Crime.

TABLE II

AUC COMPARISON OF DIFFERENT GRAPH ADJACENCY MATRIX A^F CONSTRUCTION METHODS ON UCF-CRIME.

Dyn-A1	Dyn-A2	Para-A	Csim-A	Jsim-A	AUC (%)
✓					84.67
	✓				84.38
		✓			82.89
			✓		83.68
				✓	83.27

Figure 3. The results show that with the increase of sampling length, the performance improves firstly and then decreases slightly. We observe the same trend on ShanghaiTech. We choose $T=150$ as the default setting for UCF-Crime and $T=100$ for ShanghaiTech based on the experiment.

To verify the efficiency of our proposed graph construction method of the adjacency matrix A^F , we perform ablation experiments on different construction methods. Dyn-A1 that we used is shown in Equation 1. Motivated by [26], Dyn-A2 is shown in Equation 5. Para-A denotes that the adjacency matrix is a parametric matrix, which contains N^2 parameters. Csim-A is computed by the cosine similarity scores of segment features. Inspired by [27], Jsim-A is computed by the Jaccard similarity scores of segment features. According to Table 2, dynamic construction of A^F achieves the best performance. Constructing the adjacency matrix dynamically in different ways has little effect on the model performance, but both are better than the adjacency matrix that is constructed fixedly at the beginning. If the graph structure does not depend on the input features of nodes at all, the final result is inferior, probably because the fixed design about the graph learning layer is limitative in learning.

$$A_{(i,j)} = \frac{e^2(x_i, x_j)}{\sum_{j=1}^N e^2(x_i, x_j)}, e(x_i, x_j) = (wx_i)^T wx_j \quad (5)$$

To verify the efficiency of constructing a global graph, we construct feature similarity graph and temporal consistency graph to train two independent branches and evaluate the

TABLE III
AUC COMPARISON OF DIFFERENT GRAPHS ON UCF-CRIME.

Method	AUC (%)
feature similarity graph	83.78
temporal consistency graph	83.26
late fusion	83.92
global graph	84.67

performance of late fusion by averaging the results. The performance comparison on UCF-Crime dataset is shown in Table 3. It can be observed that constructing a global graph is more capable of expressing the complex relationships coupled together among the segments.

As for the residual connection, our model can obtain a performance gain of 2.5% on UCF-Crime and 1.74% on ShanghaiTech, which demonstrates its effectiveness.

IV. CONCLUSIONS

In this work, we propose an adaptive graph convolutional network for video anomaly detection. The method constructs a global graph considering both feature similarity and temporal disparity. Moreover, a graph learning layer is introduced to construct connections among segments in a video adaptively, which can capture spatial-temporal relationships among video segments effectively and enhance current temporal features. Extensive experiments on two typical datasets show that the proposed method achieves a high level of performance for video anomaly detection.

REFERENCES

- [1] T. Xiao, C. Zhang, and H. Zha, "Learning to detect anomalies in surveillance video," *IEEE Signal Process. Lett.*, vol. 22, no. 9, pp. 1477–1481, 2015.
- [2] W. Sultani, C. Chen, and M. Shah, "Real-world anomaly detection in surveillance videos," in *Proc. IEEE Conf. Comput. Vision Pattern Recognit.*, 2018, pp. 6479–6488.
- [3] K. R. Mestav and L. Tong, "Universal data anomaly detection via inverse generative adversary network," *IEEE Signal Process. Lett.*, vol. 27, pp. 511–515, 2020.
- [4] J. Zhang, L. Qing, and J. Miao, "Temporal convolutional network with complementary inner bag loss for weakly supervised anomaly detection," in *Proc. IEEE Int. Conf. Image Process.* IEEE, 2019, pp. 4030–4034.
- [5] B. Wan, Y. Fang, X. Xia, and J. Mei, "Weakly supervised video anomaly detection via center-guided discriminative learning," in *Proc. IEEE Int. Conf. Multimedia Expo.* IEEE, 2020, pp. 1–6.
- [6] J.-C. Feng, F.-T. Hong, and W.-S. Zheng, "Mist: Multiple instance self-training framework for video anomaly detection," in *Proc. IEEE Conf. Comput. Vision Pattern Recognit.*, 2021, pp. 14 009–14 018.
- [7] S. Yu, C. Wang, Q. Mao, Y. Li, and J. Wu, "Cross-epoch learning for weakly supervised anomaly detection in surveillance videos," *IEEE Signal Process. Lett.*, vol. 28, pp. 2137–2141, 2021.
- [8] X. Wang and A. Gupta, "Videos as space-time region graphs," in *Proc. Eur. Conf. Comput. Vis.*, 2018, pp. 399–417.
- [9] L. Shi, Y. Zhang, J. Cheng, and H. Lu, "Two-stream adaptive graph convolutional networks for skeleton-based action recognition," in *Proc. IEEE Conf. Comput. Vision Pattern Recognit.*, 2019, pp. 12 026–12 035.
- [10] J. Lin, Q. Cai, and M. Lin, "Multi-label classification of fundus images with graph convolutional network and self-supervised learning," *IEEE Signal Process. Lett.*, vol. 28, pp. 454–458, 2021.
- [11] M. Feng, S. Z. Gilani, Y. Wang, L. Zhang, and A. Mian, "Relation graph network for 3d object detection in point clouds," *IEEE Trans. Image Process.*, vol. 30, pp. 92–107, 2020.
- [12] J.-X. Zhong, N. Li, W. Kong, S. Liu, T. H. Li, and G. Li, "Graph convolutional label noise cleaner: Train a plug-and-play action classifier for anomaly detection," in *Proc. IEEE Conf. Comput. Vision Pattern Recognit.*, 2019, pp. 1237–1246.
- [13] P. Wu, J. Liu, Y. Shi, Y. Sun, F. Shao, Z. Wu, and Z. Yang, "Not only look, but also listen: Learning multimodal violence detection under weak supervision," in *Proc. Eur. Conf. Comput. Vis.* Springer, 2020, pp. 322–339.
- [14] K. He, X. Zhang, S. Ren, and J. Sun, "Deep residual learning for image recognition," in *Proc. IEEE Conf. Comput. Vision Pattern Recognit.*, 2016, pp. 770–778.
- [15] J. Carreira and A. Zisserman, "Quo vadis, action recognition? a new model and the kinetics dataset," in *Proc. IEEE Conf. Comput. Vision Pattern Recognit.*, 2017, pp. 6299–6308.
- [16] D. Jayaraman and K. Grauman, "Slow and steady feature analysis: higher order temporal coherence in video," in *Proc. IEEE Conf. Comput. Vision Pattern Recognit.*, 2016, pp. 3852–3861.
- [17] S. Paul, S. Roy, and A. K. Roy-Chowdhury, "W-talc: Weakly-supervised temporal activity localization and classification," in *Proc. Eur. Conf. Comput. Vis.*, 2018, pp. 563–579.
- [18] Y. Liu, K. Wang, L. Liu, H. Lan, and L. Lin, "Tcgl: Temporal contrastive graph for self-supervised video representation learning," *IEEE Trans. Image Process.*, vol. 31, pp. 1978–1993, 2022.
- [19] H. Sapkota and Q. Yu, "Bayesian nonparametric submodular video partition for robust anomaly detection," in *Proc. IEEE Conf. Comput. Vision Pattern Recognit.*, 2022, pp. 3212–3221.
- [20] K. Liu and H. Ma, "Exploring background-bias for anomaly detection in surveillance videos," in *Proceedings of the 27th ACM International Conference on Multimedia*, 2019, pp. 1490–1499.
- [21] D. Tran, L. Bourdev, R. Fergus, L. Torresani, and M. Paluri, "Learning spatiotemporal features with 3d convolutional networks," in *Proc. IEEE Int. Conf. Comput. Vision*, 2015, pp. 4489–4497.
- [22] X. Wang, R. Girshick, A. Gupta, and K. He, "Non-local neural networks," in *Proc. IEEE Conf. Comput. Vision Pattern Recognit.*, 2018, pp. 7794–7803.
- [23] Y. Zhu and S. Newsam, "Motion-aware feature for improved video anomaly detection," *arXiv preprint arXiv:1907.10211*, 2019.
- [24] M. Z. Zaheer, A. Mahmood, H. Shin, and S.-I. Lee, "A self-reasoning framework for anomaly detection using video-level labels," *IEEE Signal Process. Lett.*, vol. 27, pp. 1705–1709, 2020.
- [25] M. Z. Zaheer, A. Mahmood, M. Astrid, and S.-I. Lee, "Claws: Clustering assisted weakly supervised learning with normalcy suppression for anomalous event detection," in *Proc. Eur. Conf. Comput. Vis.* Springer, 2020, pp. 358–376.
- [26] J. Yang, W.-S. Zheng, Q. Yang, Y.-C. Chen, and Q. Tian, "Spatial-temporal graph convolutional network for video-based person re-identification," in *Proc. IEEE Conf. Comput. Vision Pattern Recognit.*, 2020, pp. 3289–3299.
- [27] B. Fernando and S. Herath, "Anticipating human actions by correlating past with the future with jaccard similarity measures," in *Proc. IEEE Conf. Comput. Vision Pattern Recognit.*, 2021, pp. 13 224–13 233.